

<https://doi.org/10.1038/s41612-024-00620-6>

# New measurements reveal a large contribution of nitrogenous molecules to ambient organic aerosol

Check for updates

Xu Yu<sup>1,2</sup>, Qianfeng Li<sup>3</sup>, Kezheng Liao<sup>3</sup>, Yumin Li<sup>1,4</sup>, Xinming Wang<sup>5</sup>, Yang Zhou<sup>6,7</sup>, Yongmei Liang<sup>8</sup> & Jian Zhen Yu<sup>1,2,3,9</sup> ✉

Nitrogen is a significant element that constitutes ambient organic aerosol. Individual N-containing organic molecules are known to have both natural and anthropogenic sources and implicated in a wide-ranging health and environmental effects. Yet, unlike carbon (C), the total quantity of aerosol organic nitrogen (ON) remains largely unquantified, hindering a quantitative understanding of their major sources and impacts. Here, aerosol ON is quantitatively surveyed in hundreds of aerosol filter samples collected from sites of varying urban influence in China using our recently developed method that permits simple, and yet sensitive, simultaneous detection of inorganic and organic nitrogen. Annual average ON concentration was in the range of 0.4–1.4  $\mu\text{g N m}^{-3}$ , representing 17–31% of aerosol total nitrogen. Monte Carlo simulations constrained by paired ON and OC measurements suggest N-containing organic molecules contributed typically 37–50%, with a 95% confidence interval of [12%, 94%], to ambient organic aerosols. Source apportionment analysis reveals that biomass burning and secondary formation are dominant ON sources, accounting for 21–24% and ~30% of ON, respectively. Primary biological aerosol is also a significant source of ON (7–18%), with its contribution more prominent in non-urban atmospheres. The results provide the quantitative data for the extent of presence of organic nitrogenous aerosol and the origin of their major sources. Such data, we anticipate, would bring forth a breakthrough in our ability to describe and model organic aerosols and to assess their environmental impacts, such as atmospheric nitrogen nutrient inputs to ecosystems.

Atmospheric aerosols modulate the radiative forcing of the Earth and adversely affect human health<sup>1</sup>. While inorganic aerosols are well constrained benefitting from abundantly available measurements, the compositions of organic aerosol (OA), representing 20–90% of fine aerosol mass, remain uncharacterized for more than two-thirds of the OA mass<sup>2,3</sup>. In recent decades, significant progress has been made in quantifying emissions, unravelling atmospheric processes, and characterizing the compositions of

OA<sup>4–6</sup>. However, the past efforts are dominantly carbon-centered, with little attention given to the nitrogen (N) element that constitutes many of these OA molecules. Little is known about the abundance, sources, and atmospheric behaviors of nitrogenous organic aerosols (OA<sub>N</sub>)<sup>7</sup>. On the other hand, the increasing application of ultrahigh resolution mass spectrometry, which is capable of determining elemental compositions of organic molecules in complex mixture samples, has revealed the presence of hundreds of

<sup>1</sup>Division of Environment & Sustainability, Hong Kong University of Science & Technology, Hong Kong, China. <sup>2</sup>Center for Ocean Research in Hong Kong and Macau, Hong Kong University of Science & Technology, Hong Kong, China. <sup>3</sup>Department of Chemistry, Hong Kong University of Science & Technology, Hong Kong, China. <sup>4</sup>School of Environmental Science and Engineering, Southern University of Science and Technology, Shenzhen, Guangdong, China. <sup>5</sup>State Key Laboratory of Organic Geochemistry and Guangdong Key Laboratory of Environmental Protection and Resources Utilization, Guangzhou Institute of Geochemistry, Chinese Academy of Sciences, Guangzhou, China. <sup>6</sup>Frontier Science Center for Deep Ocean Multispheres and Earth System (FDOMES) and Physical Oceanography Laboratory, Ocean University of China, Qingdao, Shandong, China. <sup>7</sup>College of Oceanic and Atmospheric Sciences, Ocean University of China, Qingdao, Shandong, China. <sup>8</sup>State Key Laboratory of Heavy Oil Processing, China University of Petroleum, Beijing, China. <sup>9</sup>Fok Ying Tung Graduate Research Institute, Hong Kong University of Science & Technology, Nanshan, Guangzhou, China. ✉e-mail: [jian.yu@ust.hk](mailto:jian.yu@ust.hk)

N-containing organic molecules in ambient OA<sup>8,9</sup>. Separately, certain organic nitrogen (ON) compounds of known atmospheric presence, are light-absorbing and thus contributing to the aerosol's role in mediating climate<sup>10</sup>; some are active participants in the formation of new particles and secondary organic aerosols<sup>11,12</sup>. Last but not the least, the increasing atmospheric deposition of nitrogen from human activities has greatly disturbed the global nitrogen cycle<sup>13,14</sup>, and aerosol ON could be a significant contributor of this pool of reactive nitrogen in the atmosphere.

Existing quantitative knowledge of aerosol ON is limited to a small number of ON compound groups (e.g., urea, small amines, amino acids, nitroaromatic compounds, nitro-PAHs)<sup>15,16</sup>, or to the ON subgroups such as organic nitrates, whose mass can be quantified by aerosol mass spectrometer (AMS) or thermal dissociation couple with optical measurement (TD-LIF)<sup>17,18</sup>. The bulk ON analysis is mostly limited to the water-soluble fraction. The water-soluble ON (WSO<sub>N</sub>) is commonly measured as this sub-fraction of ON is analytically accessible via water extraction. WSO<sub>N</sub> is quantified by taking the difference between aerosol water-soluble total nitrogen (WSTN) and inorganic nitrogen (IN)<sup>7,19</sup>. The water-insoluble ON (WION) remained largely unknown, making the total quantity of aerosol ON – constituting WSO<sub>N</sub> and WION – rarely quantified. Although a few studies quantified aerosol ON by taking the difference between total N, which is measured by a Carlo Erba elemental analyzer (EA)<sup>20–23</sup>, and IN, EA fails to measure accurately trace-level aerosol nitrogen due to its unsatisfactory limit of detection for nitrogen<sup>22,23</sup>. In addition, the “difference method” brings large propagation error to ON quantification, especially when ON is a minor contributor to aerosol nitrogen<sup>24</sup>. Recently, we have developed an aerosol IN&ON analyzer that uses programmed thermo-evolution and chemiluminescent detection coupled with multivariate curve resolution data treatment to achieve sensitive and simultaneous quantification of aerosol IN and ON without any pretreatment<sup>24</sup>. The method breakthrough enables quantitative and accurate surveying of ON in a large number of samples with ease. The quantified ON represents the total N mass in OA<sub>N</sub>, which represents the sum of all nitrogen-containing molecules, including both water-soluble and water insoluble fractions. OA<sub>N</sub> encompasses oxidized OA<sub>N</sub>, such as organic nitrates and nitroaromatics, as well as reduced OA<sub>N</sub>, such as urea, amino acids, and indazoles. Therefore, the achievement of total ON determination opens the door for investigating the magnitude and sources of bulk OA<sub>N</sub>.

In this work, we applied the new method and quantified ON in more than 600 aerosol filter samples collected from multiple sites of varying urban influence in China and spanning a whole year at most sites. The relative quantities of aerosol ON and IN and their typical varying ranges in urban and suburban atmospheres are established in this study. Organic carbon (OC) and other major aerosol chemical constituents, as well as various source-specific elements and organic molecules, are also measured. The joint OC and ON data make it possible to estimate the extent of the presence of OA<sub>N</sub> in atmospheric organic aerosols, and the estimation results show a dominating importance of OA<sub>N</sub>. Source analysis further identifies biomass burning and secondary formation as major ON sources, with primary biological particle emission a prominent ON source in non-urban environments. We anticipate that the knowledge about aerosol ON quantities could be greatly valuable in bridging gaps in the description of ambient organic aerosols and in assessing the atmospheric deposition of ON in N nutrient cycle in the environment.

## Results and discussion

### Abundances of ON

Average concentrations of PM<sub>2.5</sub>-bound ON ranged from 0.4 to 1.4 μg N m<sup>-3</sup> across 12 sampling sites in China (Table 1), including two suburban sites in the North China Plain (NCP), three suburban/rural sites, and seven urban sites in the Pearl River Delta (PRD), a region in South China that includes three of China's largest cities with a total population of more than 60 million people. The percentages of ON accounting for total aerosol N were 17–31% at the sites, indicating ON represents a significant fraction of aerosol N and therefore atmospheric N deposition budget. We segregate the

12 sites into three groups – Suburban NCP, Suburban/rural PRD, and urban PRD – based on geographic locations and the degree of urban influences. Both IN and ON showed significantly higher levels in northern China than southern China ( $p < 0.0001$ ), while the ON-in-TN percentages were comparable in the two regions ( $p = 0.08$ ) (Fig. 1). Between the urban and suburban/rural site groups in the PRD region, the average of ON was slightly higher in urban areas ( $p < 0.001$ ) while the IN abundances were comparable ( $p = 0.62$ ). This makes the median of ON-to-TN ratio higher in the urban environment (22%) than in suburban/rural environment (17%) ( $p < 0.001$ ) (Fig. 1).

### Estimation of OA<sub>N</sub> contribution to OA

We next take advantage of the jointly measured OC and ON, which was achieved by our newly established method<sup>24</sup>, to estimate the contribution of nitrogenous organic aerosols (OA<sub>N</sub>) to OA. Mathematically, the fraction of OA<sub>N</sub> (i.e., the sum mass of all nitrogen-containing organic molecules) in OA can be expressed to be the products of three ratios, as shown in Eq. (1) and a simplified version in Eq. (2):

$$\frac{OA_N}{OA} = \left(\frac{OA_N}{ON}\right) \times \left(\frac{ON}{OC}\right) \times \left(\frac{OC}{OA}\right) \quad (1)$$

$$\frac{OA_N}{OA} = A \times B \times C \quad (2)$$

Where  $A$  is the OA<sub>N</sub>-to-ON ratio,  $B$  is the ON-to-OC ratio, and  $C$  is the reciprocal of OA-to-OC ratio, all in the unit of g/g. More specifically,  $A$  is the factor converting ON mass to mass of N-containing organic molecules, i.e., OA<sub>N</sub> mass. At a molecular level, this information is exactly known for individual molecules of known molecular formula (e.g., 2.14 for urea, 3.21 for ethyl amine, 9.36 for leucine, etc). Estimation of  $A$  for ambient OA can be made by assuming molecular formulas for constituent groups of OA<sub>N</sub> and their relative abundance ranges in OA<sub>N</sub> by surveying the literature, which is detailed later in this section and in Supplementary Note 2.3 and 2.5 in the supporting material.  $B$  is the N-to-C mass ratio of the bulk OA. This ratio has been measured for more than 600 ambient PM<sub>2.5</sub> aerosol samples collected in multiple sites covering urban, suburban, and rural environments in China. The reciprocal of  $C$ , better known as the OA-to-OC or organic matter (OM)-to-OC ratio in the literature<sup>25</sup>, converts OC mass to OA (or OM) mass.

We have estimated the population of possible OA<sub>N</sub>/OA values using Monte Carlo (MC) simulation to individually sample the distribution domains of the three underlying terms in Eq. (2) (see Fig. 2). Monte Carlo simulation is a powerful technique to produce the “most probable” range of a resultant variable ( $y$ ) from a number of independent variables ( $x_{i,j}$ )<sup>26</sup>. Specific to this study, OA<sub>N</sub>/OA is the resultant variable  $y$  and  $A$ ,  $B$ , and  $C$  are the three independent variables. The population distribution of  $B$  (i.e., ON/OC) is well described by the 609 samples collected from 12 continental sites. It exhibits a lognormal distribution (Fig. 2B and Supplementary Fig. 1), with a population mean of 0.11, a standard deviation of 0.06, and a median of 0.10. Such a lognormal distribution is common for concentration data of atmospheric pollutants<sup>27</sup>, and its underlying physical basis has been discussed in a few publications<sup>28–30</sup>. Mathematically, it can be proved that the division and multiplication of two lognormal random variables also yield lognormal distributions. Thus, a log-normal distribution has been adopted for all the three ratio quantities in Eq. (2).

The reciprocal of  $C$  (i.e., OA/OC) is constrained in the range of 1.3–2.5, based on the numerous past studies of organic aerosols<sup>25,31</sup> and assumed to follow a log-normal distribution (Fig. 2C). In comparison, much less information is available to deduce the distribution domain for  $A$  (i.e., OA<sub>N</sub>/ON). We constrain its distribution domain by taking a bottom-up approach, i.e., the bulk OA<sub>N</sub>/ON is calculated by summing up individual constituent groups of nitrogenous compounds (see Equation (S3)), such as urea, amino acids, etc (Supplementary Table 2), for which the converting factors of ON-to-organic compound mass are known from their chemical formulas. Due

**Table 1 | Summary information of the 12 sampling sites and sample collection details**

Environments	Sampling sites	Abbr. of sites	Locations	Sampling periods	No. of samples
Suburban, NCP <sup>a</sup>	Beijing	BJ	Beijing	04/2016–04/2017	60
	Qingdao	QD	Shandong	09/2016 & 12/2019	54
Urban, PRD <sup>a</sup>	Guangzhou	GZ	Guangdong	01/2016–12/2016	57
	Nanhai	NH	Guangdong	01/2016–12/2016	57
	Dongguan	DG	Guangdong	01/2016–12/2016	40
	Guangzhou Institute of Geochemistry	GIG	Guangdong	09/2016–08/2017	60
	Tsuen Wan	TW	Hong Kong	01/2016–12/2016	60
	Yuen Long	YL	Hong Kong	12/2016	28
	Mong Kok	MK	Hong Kong	05/2017	27
Suburban/Rural, PRD	Nansha	NS	Guangdong	01/2016–12/2016	56
	Dinghushan	DHS	Guangdong	09/2016–08/2017	60
	University of Science and Technology	UST	Hong Kong	01/2018–12/2018	60

<sup>a</sup>NCP and PRD are short for North China Plain (northern China) and Pearl River Delta (southern China), respectively.

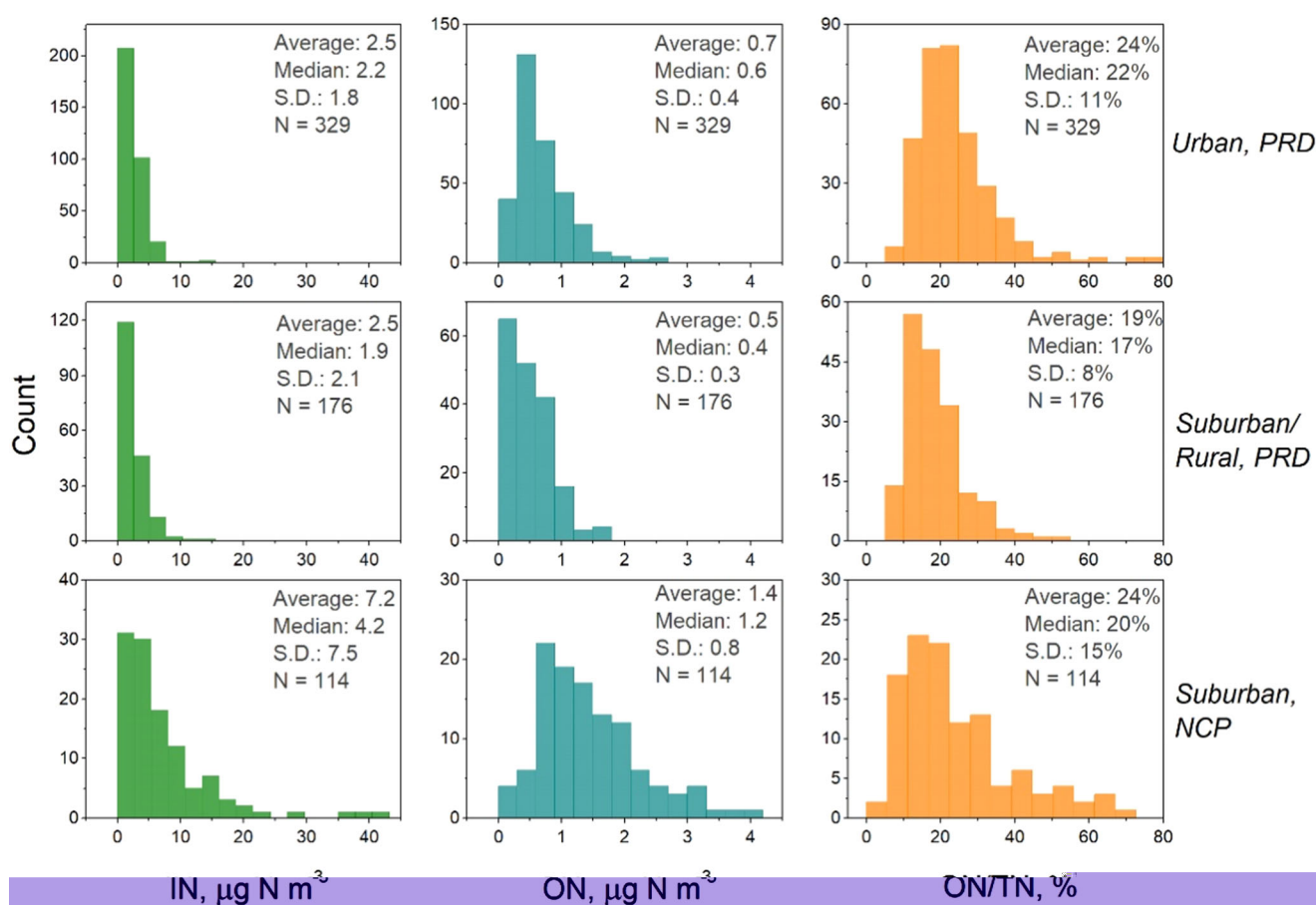


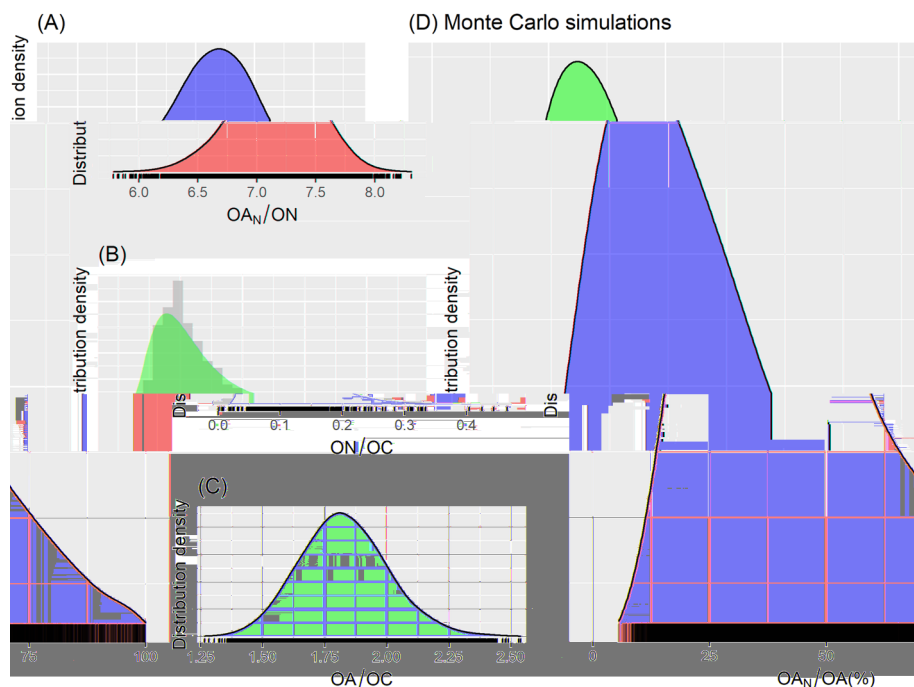
**Fig. 1 | Distribution histograms of aerosol IN and ON concentrations and ON-to-TN ratio in three groups of sampling sites in China.** Statistical data (i.e., averages, medians, and standard deviations) are presented in each plot. The 12 sampling sites

(see details in Table 1) are segregated into three groups, namely urban PRD, suburban/rural PRD, and suburban NCP.

to the complex mixture nature of  $OA_N$  and the spatiotemporal variation in abundance, MC simulations were carried out to produce the distribution in Fig. 2A. The details are provided in Supplementary Note 2 in the supplementary material. The mean of  $A$  is estimated to be 7.16, with a 95% confidence interval of [6.45, 7.78] (Fig. 2A). Namely, the mean MW of nitrogenous molecules constituting  $OA_N$  is  $\sim 100$  Da per N atom.

Based on the MC simulation of the constrained distributions of  $A$ ,  $B$ , and  $C$ , the resultant  $OA_N/OA$  ratio is estimated to have a mean of 42.2%, a median of 38.6%, and a 95% confidence interval of [14.1%, 87.3%] (Fig. 2D). Sensitivity evaluations were conducted to test if the estimated  $OA_N/OA$  can be significantly altered with different assumptions. The details of MC simulations for deriving  $OA_N/OA$  and sensitivity tests are presented in

**Fig. 2 | Distributions of three ratio quantities ( $OA_N/ON$ ,  $ON/OC$ , and  $OA/OC$ ) and the resultant  $OA_N/OA$ .** The  $OA_N/ON$  distribution is obtained by reviewing available studies on  $OA_N$  constituents and then Monte Carlo simulation (A). The  $ON/OC$  distribution is from measurements of 600+ aerosol samples, shown in grey bars in (B). The  $OA/OC$  values are constrained in the range of 1.3–2.5 and assumed to follow a log-normal distribution (C). The resultant  $OA_N/OA$  ratio is obtained based on Monte Carlo simulation of the constrained distributions of  $OA_N/ON$ ,  $ON/OC$ , and  $OA/OC$  (D).



Supplementary Note 2 in the supporting materials. A brief account is given below.

First, A and C in the MC simulations were assumed to take lognormal, normal, and triangular distributions, which produced the nearly identical means of  $OA_N/OA$  of 42.2%, 42.3%, and 42.3%, respectively (Supplementary Table 3). Second, the confidence level of numerical ranges of each variable for MC simulations was assumed at three different levels at 90%, 95%, and 99%. The resulting means of  $OA_N/OA$  ratio were nearly the same, and so were the confidence ranges of  $OA_N/OA$ , varying from [13.9%, 87.2%] at 90% confidence level to [14.3%, 87.1%] at 99% confidence level (Supplementary Table 4). These results indicate that neither the change of distribution assumption of variable nor the assumed confidence level has much influence on the estimated  $OA_N/OA$  distribution.

Third, sensitivity tests of  $OA_N/OA$  to the changes of molecular weight normalized against N atoms ( $MW_{NN}$ ) for  $OA_N$  components were conducted. The numerical ranges adopted in Supplementary Table 2 may over- or underestimate the real-world  $MW_{NN}$  of  $OA_N$  components, as their information in the literature remains partial. For the  $MW_{NN}$  of each  $OA_N$  component, a  $\pm 30\%$  change was applied individually to see the variation of  $OA_N/OA$ , as a larger percentage change may not accord with realistic situation. With all the perturbation scenarios considered, the  $OA_N/OA$  mean varied from 39.5% to 43.7% while its 95% confidence interval varied from [12.9%, 86.5%] to [14.8%, 88.5%] (Supplementary Table 5). We conducted another sensitivity test of  $MW_{NN}$  change for WION fraction since the molecular information of this part of  $OA_N$  is more uncertain than other  $OA_N$  components.  $MW_{NN}$  of all WION components were synchronously changed by  $-30\%$ ,  $-20\%$ ,  $-10\%$ ,  $+10\%$ ,  $+20\%$ ,  $+30\%$ . The MC simulation-derived  $OA_N/OA$  mean changed from 36.5% to 45.9%, with 95% confidence interval varying from [11.9%, 82.6%] to [15.7%, 90.9%] among these changes (Supplementary Table 6).

Fourth, sensitivity tests were conducted to assess the impact of changes in the percent contributions of  $OA_N$  components to the total  $OA_N$  (i.e.,  $X_i$  in Supplementary Table 2). The range for each  $X_i$  was expanded. The lower and upper bound of ranges were set as almost the lowest and highest values that were reported in previous studies. For instance, the contribution of urea to  $OA_N$  was changed from 2–10% to 0.1–20% according to the available measurements. All the ranges were expanded simultaneously in the MC simulation. As a result, the mean  $OA_N/OA$  and its 95% confidence interval vary from 42.2% and [14.1%, 87.3%] to 45.9% and [14.8%, 91.5%], respectively (Supplementary Table 7). Lastly, we tested the variation of

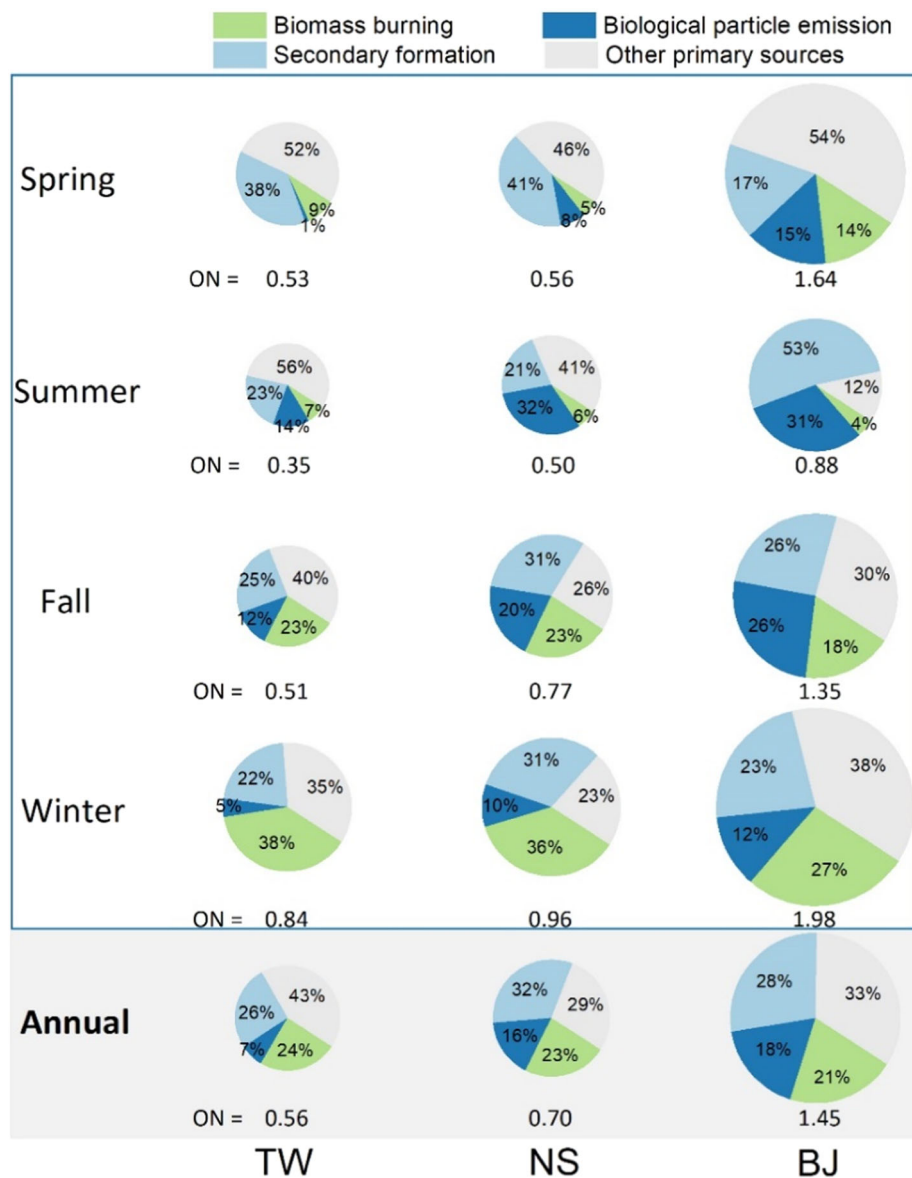
$OA_N/OA$  under the synchronous changes of  $MW_{NN}$  of the WION components and the percent contributions of each  $OA_N$  subgroup. The results suggested that the mean of  $OA_N/OA$  could vary from 40% to 49.5% and its 95% confidence interval change from [12.6%, 86.8%] to [16.2%, 93.9%] (Supplementary Table 8).

Based on the MC simulations and comprehensive sensitivity tests, we estimate that, in the environments of urban influence, the mean of  $OA_N/OA$  is  $\sim 42\%$ , likely in the range of 37–50%, while the 95% confidence interval of  $OA_N/OA$  would be [12%, 94%]. In other words, our analysis indicates that approximately one-third to one half of the OA mass is contributed by nitrogenous organic molecules (i.e.,  $OA_N$ ). The revelation of such a large presence is only made possible with our joint measurements of aerosol bulk ON and OC. This implies that N as a constituent element is widely incorporated in atmospheric organic compounds in the particle phase.

Note that there may be potential dependencies between A (i.e.,  $OA_N/ON$  ratio) and C (i.e.,  $OC/OA$  ratio) in Eq. (2), which could introduce bias in the MC simulation results of  $OA_N/OA$  mentioned earlier. To address this issue, we employed an alternative algorithm, which is more complex, to calculate  $OA_N/OA$  and conducted additional MC simulations. The detailed methodology is described in Supplementary Note 3. In the new equation (Equation (S7)) for determining  $OA_N/OA$ , all variables can be assumed to be independent of each other. Using the alternative MC simulations, we obtained a mean value of 39.8% and a median value of 37.2% for  $OA_N/OA$ , with a 95% confidence interval of [13.8%, 78.9%]. These results are quite close to the simulation scheme that ignores dependence among variables, where the mean value is 42.2%, the median value is 38.6%, and the 95% confidence interval is [14.1%, 87.3%]. Based on this comparison, we have decided to stick to the simpler numeric model presented in the main text, as it is more straightforward and easier to understand.

Our results also suggest that the mean of  $MW_{NN}$  of  $OA_N$  molecules is unlikely to exceed 109 Da per N (i.e.,  $7.78 \times 14$ , the upper bound of 95% confidence interval). For example, if the mean  $MW_{NN}$  is assigned to be 200 Da per N, the MC simulation would derive at a population distribution of  $OA_N/OA$  that has the mean at  $\sim 84\%$  and about one-quarter of  $OA_N/OA$  values in the distribution would exceed 100%, which is obviously not reasonable. This analysis implicates that most  $OA_N$  molecules are either low MW (e.g.,  $\sim 100$  Da or less) or contain more than one N atom per molecule. Such information, although crude, provides valuable hints for proposing analytical strategies in elucidating molecular composition.

**Fig. 3 | Annual and seasonal average contributions of major source groups to aerosol ON at three sites of varying urban influence in China.** The three sites include an urban site in Hong Kong (TW), a rural site in south China (NS), and a suburban site in north China (BJ). The size of pie is proportional to aerosol ON mass concentration ( $\mu\text{g N m}^{-3}$ ). Individual contributions are shown for three major source groups – biomass burning, secondary formation, and biological particle emission. A lumped source contribution is shown for other primary sources, which include industrial emission, fossil fuel combustions (coal combustion, vehicle emission, ship emission), soil dust, and sea salt. Individual contributions of these sources can be found in Supplementary Table 9.



Despite the loss of semi-volatile organic compounds during sampling would introduce biases in the measurements of OC and ON, and then the estimation of  $\text{OA}_\text{N}/\text{OA}$ , the efforts made by us have revealed a substantial presence of nitrogenous molecules in atmospheric OA. This revelation implies that the contribution of nitrogenous organic compounds to carbon chemistry may have been under-appreciated in the past. We anticipate that this newfound understanding of OA composition will inspire a reassessment of the priorities in studying and modeling OA. It is recommended that future efforts focus on integrating bulk ON measurements with the quantification of individual N-containing organic molecules. This combination of bulk analyses and speciation work would greatly enhance our ability to identify the significant constituent species of  $\text{OA}_\text{N}$  in different environments and across various seasons. Additionally, development of online ON measurement techniques would be invaluable for advancing investigations into the sources and chemical processes linked to  $\text{OA}_\text{N}$ .

### Source apportionment of ON

So far, we know little about the major sources of aerosol ON. In this study, we have gained quantitative information on the sources of aerosol ON by positive matrix factorization (PMF) analysis of a subset of the 600+ samples,

specifically those collected from urban TW, rural NS, and suburban BJ sites, which had comprehensive speciation data available (ref. Methods section). The details of PMF analysis are presented in the supporting materials (see Supplementary Note 4). The site-by-site seasonal and annual average source apportionment results are shown in Fig. 3, while the annual average statistics are tabulated in Supplementary Table 9. The PMF-resolved sources fall into two categories, namely primary and secondary sources. About 70% of aerosol ON was derived from primary emissions, including biomass burning, primary biological particles, vehicular emissions, cooking, ship emissions, soil dust, and sea salt. Among them, biomass burning was a major contributor and accounted for 21–24% ( $0.14\text{--}0.29 \mu\text{g N m}^{-3}$ ) of aerosol ON masses (Fig. 3). Previous studies have revealed that abundant N-containing molecules can be emitted from biomass burning including urea, amino acids, N-heterocyclics, and nitroaromatic compounds<sup>32,33</sup>. It was also found that biomass burning may induce a remarkable increase of bulk WSON in ambient aerosols<sup>19,32</sup>. Primary biological aerosol particle (PBAP) emission was also a significant source of aerosol ON and contributed 7.4% ( $0.04 \mu\text{g N m}^{-3}$ ), 16.3% ( $0.11 \mu\text{g N m}^{-3}$ ), and 17.6% ( $0.25 \mu\text{g N m}^{-3}$ ) to ON mass at urban TW, rural NS, and suburban BJ sites, respectively (Fig. 3). Note that a large fraction of PBAP is in coarse mode<sup>34</sup>, so that PBAP emission is expected to contribute

more to atmospheric particulate ON pool than the observation here in  $PM_{2.5}$  alone. Vehicle emission was a significant source of aerosol ON (13.6%) at the urban TW site while a minor contributor at the rural NS site (3.4%) and the suburban BJ (4.6%) (Supplementary Table 9). It has been found that many heterocyclic amines were emitted during cooking of meat and fish<sup>35</sup>. In this study, cooking emission was identified as a significant ON source (21.5%) at the suburban BJ site. We note that at TW and NS, cooking was not resolved as a separate source due to the lack of data for cooking tracers (i.e., fatty acids and cholesterol). We subsequently examined the compositional data set at two urban sites in Hong Kong (YL and MK), for which we have cooking tracer data (Supplementary Note 4). Cooking accounted for 3.5% of ON at YL and 9.0% at MK, confirming it as an ON source in environments of notable urban influence. ON from the remaining primary sources (i.e., industrial and ship emissions, coal combustion, soil dust, and sea salt) contributed, on an annual average basis for individual sources, normally below 10% to ON mass at the sites (Supplementary Table 9).

Secondary formation processes produced a large fraction of aerosol ON, at a similar annual average level of *ca* 30% for each of the three sites (Fig. 3). Note that two secondary source factors, namely sulfate-rich factor and nitrate-rich factor, are commonly resolved across all the three sites, while two secondary organic aerosol (SOA) factors are only resolved as separate sources for the BJ site. This is due to that SOA tracer data are only available for the BJ samples and their availability supports to resolve explicit SOA sources<sup>36</sup>. The nitrate-rich factor showed a significantly higher contribution to aerosol ON at BJ ( $0.103 \mu\text{g N m}^{-3}$ , 14.3%) than at TW ( $0.034 \mu\text{g N m}^{-3}$ , 5.8%) and NS ( $0.029 \mu\text{g N m}^{-3}$ , 4.3%), broadly reflecting the much higher  $\text{NO}_x$  level at the BJ site.

Although the detailed mechanisms of secondary ON aerosol formation remain unclear, it is known that particulate organic nitrates can form through reactions between organic peroxy radicals and nitric oxide (NO), as well as between alkenes and the nitrate radical ( $\text{NO}_3$ ). These pathways create plausible connections with the nitrate-rich factor, as they share the common  $\text{NO}_x$  precursor<sup>17,37</sup>. Furthermore, organic nitrate formation can also occur in the aqueous phase through non-radical reactions involving glyoxal and nitric acid<sup>38</sup>. Additionally, nitro-aromatic compounds can be produced in the atmosphere through the addition of  $\text{NO}_2$  onto the phenol molecules<sup>39</sup>. Recent laboratory studies have indicated that heterogenous reactions between  $\text{NO}_2$  and organic compounds, such as methoxyphenols and fatty acids, have potential to serve as sources of nitro-aromatic compounds<sup>40,41</sup>. ON in the sulfate-rich factor might implicate certain ON products and sulfate could be produced through the common cloud/fog processing<sup>42</sup>. For example, the reactions between carbonyls and ammonium/amines/amino acids in the aqueous phase have been established in recent years<sup>43–45</sup>. In addition, the production of N-containing organic salts by acid-base neutralization of ammonia ( $\text{NH}_3$ ) and organic acids in deliquesced aerosols may represent a significant formation pathway of secondary ON, considering the abundant presence of  $\text{NH}_3$  and organic acids in the atmosphere<sup>46</sup>. The two SOA factors resolved for the BJ samples made a combined contribution of  $0.20 \mu\text{g N m}^{-3}$  (14.3%) to aerosol ON pool at the site (Supplementary Table 9).

Seasonally, the contribution of biomass burning was the highest during the winter (27–38%), second highest in the fall (18–23%), and lowest in the summer (4–7%) at the sites (Fig. 3). This is consistent with previous studies that biomass burning is more intensive during fall-winter period in many regions of China<sup>19,47</sup>. Coal combustion also had an elevated contribution to ON during fall and winter period at the TW site (Supplementary Fig. 12). In comparison, the proportion of ON derived from PBAP emission exhibits distinctly different seasonality, with the highest occurring in the summer (14–32%) at all the three sites. Secondary ON linked with sulfate-rich factor is an important source of aerosol ON throughout the year at the TW and NS sites in southern China. At the BJ site, sulfate-rich factor represented 20.8% of aerosol ON source in the summer, significantly higher than the annual average of 6.5% (Supplementary Fig. 12). The more significant contribution of sulfate-rich factor to ON aerosol during the spring or summer periods, is consistent with the deduction above that the ON in sulfate-rich factor might be mostly derived from aqueous formation, caused by more humid air and

stronger solar radiation in the two seasons. At BJ, the contribution of biogenic SOA (ref. SOA I in Supplementary Fig. 12) to aerosol ON increased to 21.7% in the summer, while that from the anthropogenic SOA (ref. SOA II in Supplementary Fig. 12) increased to 16.1% in the winter.

We acknowledge that the lack of tracer data for cooking emissions and SOA for the samples collected at the TW and NS sites prevents us from accurately resolving the contributions of ON fractions from their respective sources or formation processes in the PMF analysis. Although our additional analyses with the aid of YL and MK data (Supplementary Note 4) indicate that cooking- and SOA formation-derived ON should not dominate the sources of ON at TW and NS, neglecting these sources introduces uncertainty into the source apportionment results. Nevertheless, our results provided quantitative understanding of aerosol ON sources, which bridged the knowledge gap regarding the geochemical processes of the organic part of N in aerosols.

### ON/OC ratios of individual ON sources

Aerosol ON/OC ratio is an essential parameter in modeling the budget and deposition flux of atmospheric ON<sup>48</sup>. The PMF receptor modeling has provided us with the ON/OC ratio data in individual ON sources, which are tabulated in Supplementary Table 9. The biomass burning source has an atomic ON/OC ratio of 0.077–0.083, showing highly consistent results from the three independent PMF analyses of TW, NS, and BJ samples. Notably, the ON/OC ratio in the PMF-derived biomass burning source profile is comparable to the experimentally determined ON/OC ratio of 0.052–0.079 that we recorded for biomass burning smoke source samples collected in simulated field burning of rice straw and sugarcane leaves<sup>49</sup>. PBAP emission has an atomic ON/OC ratio of 0.094–0.141. The mixed source of industrial emission and coal combustion has an atomic ON/OC ratio of 0.046–0.067, and the ratios of vehicle and ship emissions are 0.048–0.076 and 0.036–0.052, respectively. Soil dust shows a relatively higher atomic ON/OC ratio of 0.129–0.162, consistent with the study by Wang et al. that documented an increased WSON/WSOC ratio during dust events compared with normal days<sup>50</sup>. Generally, ON/OC ratios in primary particles from fossil fuel combustion are relatively lower than those from natural sources such as PBAP emission and soil dust. Cooking emission profile derived from the BJ samples shows an atomic ON/OC ratio of 0.291, while a much lower value of 0.052 is obtained with the Hong Kong samples. The notable difference might result from different cooking styles at the two places and more measurements of cooking source emissions are suggested for future studies. SOA linked with the nitrate-rich factor shows a large range of atomic ON/OC ratio of 0.035–0.241 at the three sites. In comparison, SOA linked with the sulfate-rich factor process shows relatively consistent values in the range of 0.097–0.136 in southern and northern China. The two SOA factors resolved from the BJ samples have the ON/OC ratio of 0.103 and 0.082, respectively (Supplementary Table 9). Further studies in different atmospheric environments are needed to uncover the chemical compositions of secondary ON aerosol and to map out the ON/OC variation range.

Kanakidou et al.<sup>48</sup> presented the first estimate of the atmospheric budget and deposition flux of WSON to oceans relying on OC emission inventory supplemented with assumed ON/OC ratios and solubilities of OC for individual sources. In their study, an ON/OC atomic ratio of 0.3 was adopted for all combustion-sourced primary OC particles, which is notably higher than our results (*ca* 0.04–0.08) derived from PMF modeling of observational data shown in Supplementary Table 9. An ON/OC atomic ratio of 0.15 was selected for primary biogenic particles in that study, which is slightly higher than the upper bound of the range of 0.094–0.141 derived in our work. For the soil dust source, our resolved ON/OC atomic ratio (0.13–0.16) is moderately higher than the assumed ratio of 0.1 for soil microbial biomass in Kanakidou et al.<sup>48</sup>. Soil dust may include complex materials such as decomposed biomass, deposited atmospheric particles, and applied fertilizer. We note that the ON/OC ratios derived from the PMF-resolved source profiles represent bulk measurements and provide an averaged representation of elemental compositions of C and N in each source. Kanakidou et al.<sup>48</sup> applied a mean N/C ratio of 0.1 for SOA produced

by gas-to-particle conversion, which is approximately in the middle of the range of N/C ratio resolved for the four secondary sources of ON in our work (0.035–0.241). Our study, however, revealed that the secondary ON could have multiple formation pathways that produce a wide range of N/C ratio. One single value would certainly be too coarse a representation in modeling secondary  $OA_N$ . As secondary formation is a major  $OA_N$  source, more targeted laboratory and field studies are needed to characterize the ON/OC ratio. Note that the calculated ON/OC ratio for each source resolved from the PMF analysis may be subject to biases. Nevertheless, our findings provide valuable references for modeling studies of investigating N cycles and the related environmental impacts, considering the challenges associated with obtaining organic N/C ratios of emission sources.

## Methods

### Sampling

$PM_{2.5}$  samples were collected from a total of 12 sites under varying urban influence in China. The locations, as well as sampling periods at each site, are presented in Table 1 and Supplementary Fig. 19. Supplementary Fig. 19 also presents the geomorphologic maps of the sampling sites, indicating the rough distances of the sampling sites away from urban centers. Quartz fiber filter samples were collected using high-volume samplers at each of the sites. Teflon filter samples were concurrently collected using mid-volume samplers at the sites except for QD, GIG, and DHS sites. Among the 12 sites, three sites (TW, NS, and BJ) had comprehensive chemical composition data for samples covering a year, providing opportunities for source apportionment by receptor modeling with year-round samples. More descriptions of TW, NS, and BJ sites are therefore provided here. TW (Tsuen Wan) is an urban site in Hong Kong in a mixed commercial/residential neighborhood. NS (Nansha) is in a suburban/rural peripheral district of the Guangzhou municipality in southern China. The BJ (Beijing) site is on the roof of a building on the campus of China University of Petroleum, located in a suburban district of Beijing on its northwest outskirts. Sampling inlets at the three sites were all ~20 m above the ground. All samplers were calibrated before and after sampling. Field blanks were also collected at each site. All samples were immediately transferred to laboratories and stored at  $-20\text{ }^{\circ}\text{C}$  before analysis. The samples were shipped with blue ice packs to keep them cool ( $\sim 4\text{ }^{\circ}\text{C}$ ) during transport. To assess the effects of long-term storage on the chemical compositions of filter samples, we examined the consistency of IN concentrations measured by ion chromatography soon after sample collection, and by the aerosol IN&ON analyzer, conducted two to four years later in 2020. As depicted in Supplementary Fig. 20, a strong correlation ( $R^2 = 0.96$ ) was observed between the two independent sets of IN measurements, suggesting little alteration in aerosol IN species during storage.

### Chemical analysis

All the samples were analyzed for ON, IN, OC, elemental carbon (EC), and major ions. Additional measurements of elemental and organic source markers were carried out for the samples collected at BJ, TW, NS, YL, and MK sites. Non-polar organic compounds (NPOCs) and sugars were measured for the TW and NS samples, while more comprehensive measurements, including NPOCs, sugars, fatty acids, sterol, and secondary organic aerosol (SOA) tracers, were available for BJ, YL, and MK sites. The comprehensive compositional data at BJ, TW, NS, YL, and MK allowed source apportionment analysis of ON by positive matrix factorization (PMF) receptor model. All analyses are detailed in Supplementary Note 1 in the supporting materials.

### Monte Carlo simulation

Monte Carlo simulation is a computational approach that relies on repeated random sampling to solve problems that might be deterministic in principle<sup>26</sup>. Commonly, Monte Carlo simulation consists of the following steps: (1) Define a domain of input variables; (2) Generate inputs randomly from a probability distribution (e.g., normal or lognormal distributions) over the domain; (3) Perform a deterministic computation on the inputs; and (4) Aggregate the results. The simulation specifics tailored for this study are detailed in supplementary materials (Supplementary Note 2).

### Positive matrix factorization

The sources of aerosol ON were identified and resolved using EPA positive matrix factorization (PMF) receptor model version 5.0. The PMF model is a multivariate factor analysis tool based on chemical mass balance. The detailed instructions of the PMF model can be found in previous studies<sup>31,36</sup>, and it has been widely applied in the source apportionments of ambient  $PM_{2.5}$ <sup>19,31,36,45</sup>. The detailed PMF runs (e.g., input variables, interpretability of resolved source profiles, and result validations) for aerosol ON source apportionment are presented in Supplementary Note 4.

### Data availability

Ambient measurement data used in this study are available in the data repository maintained by HKUST<sup>51</sup>.

Received: 12 October 2023; Accepted: 7 March 2024;

Published online: 15 March 2024

## References

1. Yang, G. H. et al. Rapid health transition in China, 1990–2010: findings from the Global Burden of Disease Study 2010. *Lancet* **381**, 1987–2015 (2013).
2. Robinson, A. L. et al. Rethinking organic aerosols: semivolatile emissions and photochemical aging. *Science* **315**, 1259–1262 (2007).
3. Zhang, Q. et al. Ubiquity and dominance of oxygenated species in organic aerosols in anthropogenically-influenced Northern Hemisphere midlatitudes. *Geophys. Res. Lett.* **34**, 6 (2007).
4. Odum, J. R. et al. Gas/particle partitioning and secondary organic aerosol yields. *Environ. Sci. Technol.* **30**, 2580–2585 (1996).
5. Ervens, B., Turpin, B. J. & Weber, R. J. Secondary organic aerosol formation in cloud droplets and aqueous particles (aqSOA): a review of laboratory, field and model studies. *Atmos. Chem. Phys.* **11**, 11069–11102 (2011).
6. Chang, X. et al. Full-volatility emission framework corrects missing and underestimated secondary organic aerosol sources. *One Earth* **5**, 403–412 (2022).
7. Cape, J. N., Cornell, S. E., Jickells, T. D. & Nemitz, E. Organic nitrogen in the atmosphere — Where does it come from? A review of sources and methods. *Atmos. Res.* **102**, 30–48 (2011).
8. Lin, P., Rincon, A. G., Kalberer, M. & Yu, J. Z. Elemental composition of HULIS in the pearl river delta region, china: results inferred from positive and negative electrospray high resolution mass spectrometric data. *Environ. Sci. Technol.* **46**, 7454–7462 (2012).
9. Wang, X. K. et al. Chemical characteristics of organic aerosols in shanghai: a study by ultrahigh-performance liquid chromatography coupled with orbitrap mass spectrometry. *J. Geophys. Res. Atmos.* **122**, 11703–11722 (2017).
10. Laskin, A., Laskin, J. & Nizkorodov, S. A. Chemistry of atmospheric brown carbon. *Chem. Rev.* **115**, 4335–4382 (2015).
11. Yao, L. et al. Atmospheric new particle formation from sulfuric acid and amines in a Chinese megacity. *Science* **361**, 278–281 (2018).
12. Rollins, A. W. et al. Evidence for NO<sub>x</sub> Control over Nighttime SOA Formation. *Science* **337**, 1210–1212 (2012).
13. Duce, R. A. et al. Impacts of atmospheric anthropogenic nitrogen on the open ocean. *Science* **320**, 893–897 (2008).
14. Ren, H. J. et al. 21st-century rise in anthropogenic nitrogen deposition on a remote coral reef. *Science* **356**, 749–752 (2017).
15. Chow, K. S., Huang, X. H. H. & Yu, J. Z. Quantification of nitroaromatic compounds in atmospheric fine particulate matter in Hong Kong over 3 years: field measurement evidence for secondary formation derived from biomass burning emissions. *Environ. Chem.* **13**, 665–673 (2016).
16. Jickells, T., Baker, A. R., Cape, J. N., Cornell, S. E. & Nemitz, E. The cycling of organic nitrogen through the atmosphere. *Philos. Trans. R. Soc. Lond. B Biol. Sci.* **368**, 20130115 (2013).

17. Xu, W. Q. et al. Estimation of particulate organic nitrates from thermodenuder–aerosol mass spectrometer measurements in the North China Plain. *Atmos. Meas. Tech.* **14**, 3693–3705 (2021).
18. Rollins, A. W. et al. Real time in situ detection of organic nitrates in atmospheric aerosols. *Environ. Sci. Technol.* **44**, 5540–5545 (2010).
19. Yu, X. et al. Water soluble organic nitrogen (WSON) in ambient fine particles over a megacity in south China: Spatiotemporal variations and source apportionment. *J. Geophys. Res. Atmos.* **122**, 13,045–13,060 (2017).
20. Miyazaki, Y., Kawamura, K. & Sawano, M. Size distributions of organic nitrogen and carbon in remote marine. *Geophys. Res. Lett.* **37**, L06803 (2010).
21. Pavuluri, C. M., Kawamura, K. & Fu, P. Q. Atmospheric chemistry of nitrogenous aerosols in northeastern Asia: biological sources and secondary formation. *Atmos. Chem. Phys.* **15**, 9883–9896 (2015).
22. Duan, F. K., Liu, X. D., He, K. B. & Dong, S. P. Measurements and characteristics of nitrogen-containing compounds in atmospheric particulate matter in Beijing, China. *Bull. Environ. Contam. Toxicol.* **82**, 332–337 (2009).
23. Zhang, Q. et al. Organic nitrogen in PM<sub>2.5</sub> in Beijing. *Front. Environ. Sci. Eng.* **9**, 1004–1014 (2015).
24. Yu, X. et al. Simultaneous determination of aerosol inorganic and organic nitrogen by thermal evolution and chemiluminescence detection. *Environ. Sci. Technol.* **55**, 11579–11589 (2021).
25. Philip, S. et al. Spatially and seasonally resolved estimate of the ratio of organic mass to organic carbon. *Atmos. Environ.* **87**, 34–40 (2014).
26. Schwartz, L. M. Random error propagation by Monte Carlo simulation. *Anal. Chem.* **47**, 963–964 (1975).
27. Seinfeld, J. H. & Pandis, S. N. *Atmospheric Chemistry and Physics: From Air Pollution to Climate Change*. John Wiley & Sons, 2016.
28. Andersson, A. Mechanisms for log normal concentration distributions in the environment. *Sci. Rep.* **11**, 16418 (2021).
29. Kahn, H. D. Note on the distribution of air pollutants. *J. Air Poll. Ctrl. Assoc.* **23**, 973–973 (1973).
30. Ott, W. R. A physical explanation of the lognormality of pollutant concentrations. *J. Air Waste Manag. Assoc.* **40**, 1378–1383 (1990).
31. Huang, R. J. et al. High secondary aerosol contribution to particulate pollution during haze events in China. *Nature* **514**, 218–222 (2014).
32. Mace, K. A., Artaxo, P. & Duce, R. A. Water-soluble organic nitrogen in Amazon Basin aerosols during the dry (biomass burning) and wet seasons. *J. Geophys. Res.* **108**, 4512 (2003).
33. Wang, Y. J. et al. Molecular characterization of nitrogen-containing organic compounds in humic-like substances emitted from straw residue burning. *Environ. Sci. Technol.* **51**, 5951–5961 (2017).
34. Pöschl, U. et al. Rainforest aerosols as biogenic nuclei of clouds and precipitation in the Amazon. *Science* **329**, 1513–1516 (2010).
35. Sugimura, T. et al. Heterocyclic amines: Mutagens/carcinogens produced during cooking of meat and fish. *Cancer Sci.* **95**, 290–299 (2004).
36. Wang, Q. Q. et al. Impact of Secondary Organic Aerosol Tracers on Tracer-Based Source Apportionment of Organic Carbon and PM<sub>2.5</sub>: A Case Study in the Pearl River Delta, China. *ACS Earth Space Chem.* **1**, 562–571 (2017).
37. Ng, N. L. et al. Nitrate radicals and biogenic volatile organic compounds: oxidation, mechanisms, and organic aerosol. *Atmos. Chem. Phys.* **17**, 2103–2162 (2017).
38. Lim, Y. B. et al. Photochemical organonitrate formation in wet aerosols. *Atmos. Chem. Phys.* **16**, 12631–12647 (2016).
39. Wang, Y. J. et al. The formation of nitro-aromatic compounds under high NO<sub>x</sub> and anthropogenic VOC conditions in urban Beijing, China. *Atmos. Chem. Phys.* **19**, 7649–7665 (2019).
40. Li, P. et al. Inorganic ions enhance the number of product compounds through heterogeneous processing of gaseous NO<sub>2</sub> on an aqueous layer of acetosyringone. *Environ. Sci. Technol.* **56**, 5398–5408 (2022).
41. Deng, H. F. et al. Effect of Inorganic Salts on N-Containing Organic Compounds Formed by Heterogeneous Reaction of NO<sub>2</sub> with Oleic Acid. *Environ. Sci. Technol.* **55**, 7831–7840 (2021).
42. Yu, J. Z., Huang, X. F., Xu, J. H. & Hu, M. When aerosol sulfate goes up, so does oxalate: Implication for the formation mechanisms of oxalate. *Environ. Sci. Technol.* **39**, 128–133 (2005).
43. Galloway, M. M. et al. Glyoxal uptake on ammonium sulphate seed aerosol: reaction products and reversibility of uptake under dark and irradiated conditions. *Atmos. Chem. Phys.* **9**, 3331–3345 (2009).
44. Noziere, B., Dziedzic, P. & Cordova, A. Products and kinetics of the liquid-phase reaction of glyoxal catalyzed by ammonium ions (NH<sub>4</sub><sup>+</sup>). *J. Phys. Chem. A* **113**, 231–237 (2009).
45. Zhang, G. H. et al. High secondary formation of nitrogen-containing organics (NOCs) and its possible link to oxidized organics and ammonium. *Atmos. Chem. Phys.* **20**, 1469–1481 (2020).
46. Paciga, A. L., Riipinen, I. & Pandis, S. N. Effect of ammonia on the volatility of organic diacids. *Environ. Sci. Technol.* **48**, 13769–13775 (2014).
47. Ding, X. et al. Significant increase of aromatics-derived secondary organic aerosol during fall to winter in China. *Environ. Sci. Technol.* **51**, 7432–7441 (2017).
48. Kanakidou, M. et al. Atmospheric fluxes of organic N and P to the global ocean. *Glob. Biogeochem. Cycles* **26**, GB3026 (2012).
49. Lin, P., Huang, X. F., He, L. Y. & Yu, J. Z. Abundance and size distribution of HULIS in ambient aerosols at a rural site in South China. *J. Aerosol Sci.* **41**, 74–87 (2010).
50. Wang, G. H. et al. Impact of Gobi desert dust on aerosol chemistry of Xi'an, inland China during spring 2009: differences in composition and size distribution between the urban ground surface and the mountain atmosphere. *Atmos. Chem. Phys.* **13**, 819–835 (2013).
51. Yu, X. & Yu, J. Z. Aerosol Nitrogen and Carbon Observation Data at 12 sites of China [Dataset]. DataSpace@HKUST. <https://doi.org/10.14711/dataset/NZEFQG>, (2024).

## Acknowledgements

This study was supported by the Research Grants Council of Hong Kong (16307820, 16213222, 16304519, and AoE/P-601/23-N) and the Center for Ocean Research in Hong Kong and Macau, a joint research center for ocean research between Laoshan Laboratory and HKUST (QNL20SC01-T). We thank past and present Yu's group members for sample collection and chemical analysis of PM<sub>2.5</sub> constituents.

## Author contributions

X.Y., Q.F.L. and J.Z.Y. wrote the manuscript. J.Z.Y. conceived the research. X.Y. and Y.M.L. conducted the lab analyses and data processing. Q.E.L. and K.Z.L. performed Monte Carlo simulations. X.Y. carried out the ON source apportionment analysis by PMF receptor model. X.M.W., Y.Z. and Y.M.L. contributed to sample collections and discussion.

## Competing interests

The authors declare no competing interests.

## Additional information

**Supplementary information** The online version contains supplementary material available at <https://doi.org/10.1038/s41612-024-00620-6>.

**Correspondence** and requests for materials should be addressed to Jian Zhen Yu.

**Reprints and permissions information** is available at <http://www.nature.com/reprints>

**Publisher's note** Springer Nature remains neutral with regard to jurisdictional claims in published maps and institutional affiliations.



**Open Access** This article is licensed under a Creative Commons Attribution 4.0 International License, which permits use, sharing, adaptation, distribution and reproduction in any medium or format, as long as you give appropriate credit to the original author(s) and the source, provide a link to the Creative Commons licence, and indicate if changes were made. The images or other third party material in this article are included in the article's Creative Commons licence, unless indicated otherwise in a credit line to the material. If material is not included in the article's Creative Commons licence and your intended use is not permitted by statutory regulation or exceeds the permitted use, you will need to obtain permission directly from the copyright holder. To view a copy of this licence, visit <http://creativecommons.org/licenses/by/4.0/>.

© The Author(s) 2024